

Scanning internal probe for plasma particle, fluctuation, and LIF tomographic measurements

Costel Biloiu,^{a)} Earl Scime, Xuan Sun, and Brendan McGeehan
Physics Department, West Virginia University, Morgantown, West Virginia 26506-6315

(Presented on 22 April 2004; published 20 October 2004)

An internal scanning probe capable of spatially resolved measurements throughout a horizontal (r, z) cross section of the expansion region between a helicon plasma source and an expansion chamber is described. For complete diagnosis of the expanding magnetoplasma, the probe is designed to simultaneously measure the electron temperature, the electron density, the plasma potential, the magnetic fluctuation spectrum in three dimensions, and the two-dimensional ion velocity distribution function (through a tomographic inversion method). The probe design and operational characteristics as well as representative measurements are presented. © 2004 American Institute of Physics. [DOI: 10.1063/1.1787576]

An internal scanning probe has been designed to perform simultaneous measurements of the electron temperature, the electron density, the plasma potential, the magnetic fluctuation spectrum in three dimensions, and the two-dimensional ion velocity distribution function (IVDF) in the expansion region between a steady state, high density, helicon plasma source, Hot helicon experiment (HELIX), and a large diffusion chamber, large experiment on instabilities and anisotropies (LEIA).¹ Briefly, the helicon plasma source consists of a 60-cm-long Pyrex tube, 10 cm in diameter, connected to a 90-cm-long, 15-cm-diam, grounded stainless steel tube. The plasma is generated by coupling 6–18 MHz rf power (≤ 2 kW) through a Π -type matching network to a 19-cm-long, external, $m=+1$, helical antenna. Ten electromagnets capable of producing a steady state axial magnetic field up to 1100 G are responsible for plasma confinement. Argon is typically used as the working gas and characteristic argon plasma parameters are: $T_e \approx 4$ –12 eV and $n \approx (1-100) \times 10^{11} \text{ cm}^{-3}$. The HELIX plasma expands in the LEIA diffusion chamber (see Fig. 1); a 4.5-m-long, 1.8-m-inner diam, grounded aluminum chamber. The system is pumped differentially and the pressure in the diffusion chamber is approximately one order of magnitude lower than in the source. An axial, steady state magnetic field of 0–70 G is produced in LEIA by seven external electromagnets. The magnetic field gradient in the expansion region is roughly 1000 G/m.

The probe was designed to obtain spatially resolved measurements throughout a horizontal plane 100 cm in length along the z axis and 40 cm wide in the radial direction. As shown in Fig. 1, the measurement area begins in the divergent magnetic field region near the HELIX-LEIA junction and extends to the middle of the LEIA chamber. The backbone of the probe is a 6-ft-long, 3/4-in.-o.d. stainless steel shaft with 0.083-in.-thick walls that is supported by a

stainless steel ball joint bearing mounted on the interior of the feedthrough flange. The bearing is captured in a stainless steel ring supported on a 1/2 in. threaded shaft. The ring is free to rotate around the axis of the threaded shaft. Two linear motion bearings mounted on a fixed 1-in.-o.d. guide shaft align and support the heavy probe shaft as it passes through a double o-ring sliding seal. The double o-ring sliding seal consists of a modified 3/4-in. Cajon™ fitting with two Viton™ o-rings separated by an intermediate vacuum region evacuated through a 1/4 in. port. In combination with the ball joint bearing and the rotating supporting shaft, a welded bellows provides for $\pm 35^\circ$ of angular motion of the probe. The feedthrough flange and vacuum seals are described in detail in Ref. 2.

Placement of the probe shaft in the z - r plane is accomplished by two computer-driven VELMEX™ stepping motor assemblies that control the insertion depth of the probe and the tilt angle between the probe and the chamber axis. A rotary stepping motor spins the probe shaft around its axis to switch between parallel and perpendicular (with respect to the magnetic field) laser induced fluorescence (LIF) measurements and for optical tomography. The spatial and angular resolutions are determined by the precision of the stepping motors and are ≈ 1 mm and $\approx 0.5^\circ$, respectively.

The diagnostic complement mounted on the probe head [Fig. 2(a)] includes: LIF optics,^{3–5} a rf compensated cylindrical Langmuir probe⁶ and a three-dimensional (3D) magnetic sense coil array.⁷ Our previous internal LIF probe suffered from poor signal to noise, was limited to scans along a single radial chord, and was solely a LIF probe.⁸ To improve the LIF signal to noise, this probe includes optimized collection optics including light baffles, an easily aligned and replaceable mirror for laser injection, and an integrated photomultiplier tube (PMT) detector.

For argon ion LIF, laser light from a single-mode tunable ring dye laser (Coherent 899, rhodamine 6G dye) pumped by a 6 W argon-ion laser (Coherent Innova 300) is modulated at ≈ 3 kHz with a mechanical chopper, transmitted from a remote laser facility by fiber optic (≈ 10 m away), and coupled

^{a)} Author to whom correspondence should be addressed; electronic mail: costel.biloiu@mail.wvu.edu

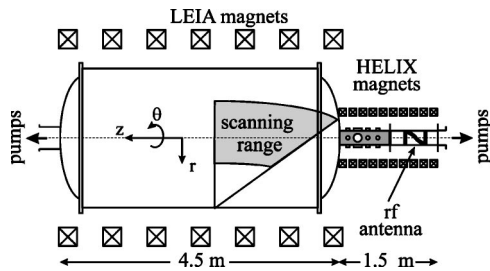


FIG. 1. The combined HELIX-LEIA system with the region accessible with the scanning probe shaded in gray.

into the internal injection 200 μm fused silica fiber through a fiber-fiber vacuum feedthrough. The injection fiber is terminated with a 1/4 in. collimating lens to create a weakly divergent beam that reflects from a plane mirror and passes 5 cm in front of the collection optics [Fig. 2(b)]. The power of the final scanning probe beam is approximately 40% of the output power of the ring dye laser. To ensure proper alignment of the injection and collection optics, the probe head was machined from a single piece of stainless steel. Before final cutting, the injection optics shafts and mirror mount were mechanically aligned to the probe head with a jig and the injection optics shafts welded into place. Then the pockets for the collection optics and the Langmuir probe were machined into the probe head.

The 2.54-cm-diam collection optics consists of a 5 cm focal length collection lens followed by a 5 cm focal length focusing lens. The numerical aperture (NA) of the focusing lens was chosen to match the numerical aperture of the 1-mm-core-diam, 2-m-long, fused silica collection fiber (NA = 0.22). Between the focusing lens and the collection fiber, a series of circular apertures [Fig. 2(b)] prevent off-axis rays from passing through the lenses and into the collection fiber. Because the plasma emits strongly at the fluorescence wavelength, reduction of background light is critical to improving the measurement signal to noise. To avoid loss of fluorescence light at another fiber-fiber vacuum feedthrough, the collected light is coupled into a Hamamatsu HC124-06 PMT⁹ mounted on the end of the probe shaft. Light exiting

the collection fiber is collimated inside the probe, passes through a standard quartz fused silica window, a 1-nm-wide interference filter (centered around 461 nm) and into the PMT. The PMT moves with the probe as it scans through the measurement plane in LEIA. The PMT signal is composed of fluorescence radiation, electron impact induced radiation and electronic noise. A Stanford Research SR830 lock-in amplifier, referenced to the modulation signal from the mechanical chopper, is used to eliminate all noncorrelated signals. Lock-in amplification is indispensable since the electron-impact induced emission is several orders of magnitude larger than the fluorescence signal. The electronically filtered LIF signal (and correlated noise) is sent to a digitizer for storage and later data analysis.

During a typical LIF measurement of the Ar II ion velocity distribution function (IVDF), from which the Ar II bulk velocity and ion temperature can be determined, approximately 200 mW of 611.49 nm (air wavelength) laser light pumps the Ar II 3d²G_{9/2} metastable state to the 4p²F_{7/2} state, which then fluoresces by emitting 460.96 nm photons. The laser frequency is swept over 20 GHz and the detected signal is recorded. Signal-to-noise levels from this probe are typically greater than 50:1 and, in contrast to our previous internal LIF probe, LIF measurements can be performed for the entire range of operational neutral pressures in the plasma source (1–20 mTorr). During each scan of the laser, 10% of the dye laser light is passed through an iodine cell¹⁰ and the iodine fluorescence recorded. The spectrum of molecular iodine lines provides a means of compensating for laser drift and of measuring the absolute velocity of the argon ions. Ion temperatures are inferred from the Doppler broadening of the absorption line.^{3–5} For the plasma and magnetic field parameters of LEIA, Stark broadening, Zeeman splitting, and the natural linewidth of the absorption line are ignorable.

By rotating the probe about its axis, the complete two-dimensional (2D) ion velocity space distribution function (parallel and perpendicular to the magnetic field) can be acquired via optical tomography.^{11,12} A collection of one-dimensional LIF scans at different injection angles relative to the external magnetic field is processed by a filtered back projection method to give a complete 2D reconstruction of the velocity distribution. Since a complete set of scans spans only 180°, the injection optics is rotated in the quadrants where it does not block the plasma flow, i.e., ±90° from the position where the injection optic faces the helicon source. A surface plot of the 2D ion velocity distribution obtained through tomographic inversion of 36 scans is shown in Fig. 3(a). The same data plotted as contours of constant $f_i(v_{||}, v_{\perp})$ are shown in Fig. 3(b). The outermost contour includes two symmetric features, each at a well defined angle to the magnetic field [the parallel direction in Fig. 3(b)]. When ions are perpendicularly heated in a nonuniform magnetic field and then flow into a region of weaker magnetic field, magnetic moment conservation requires the conversion of perpendicular kinetic energy into parallel kinetic energy. The resultant distortion of the IVDF at the highest perpendicular energies yields contours of constant $f_i(v)$ such as those shown in Fig.

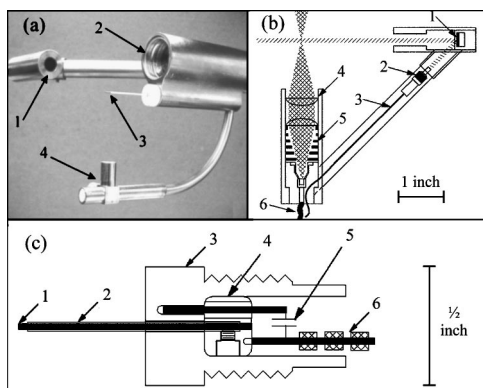


FIG. 2. Scanning probe head diagnostics: (a) 1—LIF injection optics; 2—LIF collection optics; 3—rf compensated Langmuir probe; 4—3D magnetic sense coil array. (b) 1— injection mirror; 2—collimating injection optic; 3— injection fiber; 4—collection lens; 5—light baffles; 6—collection fiber. (c) 1—0.5 mm graphite rod; 2—alumina tube; 3—boron nitride cap; 4—brass slug; 5—10 nF shorting capacitor; 6—rf choke chain.

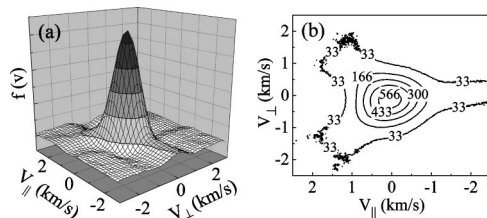


FIG. 3. Tomographic reconstruction of the 2D ion velocity distribution function as surface plot (a) and as contours of constant $f_i(v_{\parallel}, v_{\perp})$ (b).

3(b) and the “v-shaped” contours are called ion conics.¹³ Note that the signal to noise of the IVDF measurement in Fig. 3 is greater than 200:1.

Measurements of the plasma density, electron temperature, and floating potential are accomplished with a rf compensated, cylindrical Langmuir probe.⁶ To withstand the intense thermal environment of a steady state helicon plasma, the probe consists of a 0.5-mm-diam graphite rod, standard mechanical pencil graphite, surrounded by an alumina tube, 3 mm of the graphite protrudes from the alumina tube for particle collection. Electrical connection to the probe tip and the rf compensating electronics is made through a brass slug, to which the graphite rod, alumina tube, 10 nF shorting capacitor, and rf chokes are attached [Fig. 2(c)]. One lead of the shorting capacitor nearly penetrates the boron nitride shield of the probe and serves to short out high frequency electrostatic fluctuations that are picked up by the graphite tip. A series of five Lenox–Fugle rf chokes,¹⁴ covering the frequency range 6–18 MHz, provide additional rf rejection between the probe tip and the Keithley 2400 Sourcemeter used to sweep the probe tip voltage from –20 to +50 V. High pressure bulkhead mount BNC fittings, modified for high vacuum use, are used as signal feedthroughs for the Langmuir probe and the magnetic sense coils at the sealed end of the scanning probe. Typical maps of plasma density (n_e), electron temperature (T_e), and plasma potential (V_p) obtained with the scanning probe are shown in Figs. 4(a)–4(c). Since a well defined knee in the current–voltage characteristic at the plasma potential is difficult to obtain with a cylindrical probe in a high density plasma,¹⁵ the plasma potential is

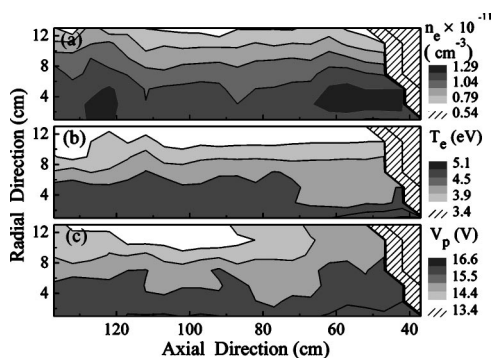


FIG. 4. Two-dimensional maps of plasma density (a), electron temperature (b), and plasma potential (c). Hatched regions are inaccessible by the scanning probe; the junction between the HELIX and LEIA chamber is at $z=0$.

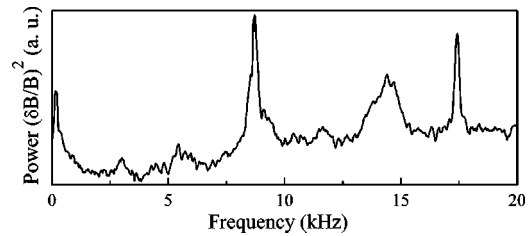


FIG. 5. Magnetic fluctuation power spectrum obtained with one of the three coils in the magnetic sense coil array.

estimated from the expression $V_p = V_f + 5.4T_e$.¹⁶ Along the axis of the expansion region, the plasma density is practically constant while T_e and V_p decrease slightly. In the radial direction, there is a sharp decrease in both n_e and T_e .

Measurement of the spectrum and amplitude of electromagnetic fluctuations over the frequency range 1–100 kHz in the expanding helicon source plasma was another design goal of the scanning probe. Each of the three magnetic sense coils is made from 300 turns of 40 HML gauge, coated copper wire (MWS Wire Industries) wound on a 7-mm-long, 3-mm-diam boron nitride reel. The sense coils are enclosed in three, mutually perpendicular cylinders machined from a single block of stainless steel and welded to the end of a precision 90° bend of 1/4 in. stainless steel tubing that was welded to the main probe head. Electrostatic shielding along the axis of each coil is accomplished with a thin piece of aluminum foil placed under the protective boron nitride cap. Signals from both leads of the coils are low-pass filtered at 100 kHz with a 16 channel, differential amplifier and recorded with a 200 kHz, 16 channel, 16 bit digitizer (Tektronix VX4780 and VX4244, respectively). A typical magnetic fluctuation power spectrum from 1 to 20 kHz is shown in Fig. 5. The spectrum is an average of 50 sets of 8192 point measurements. Evident in the spectrum is a strong electromagnetic wave at 7.4 kHz and its harmonic at 14.8 kHz. A different wave at 17.5 kHz is also visible in the spectrum. Preliminary analysis suggests that the lower frequency wave is a resistive drift wave,¹⁷ while the origin of the higher frequency wave is unknown at this time.

¹M. M. Balkey *et al.*, *Plasma Sources Sci. Technol.* **10**, 284 (2001).

²E. E. Scime *et al.*, *Rev. Sci. Instrum.* **73**, 1970 (2002).

³R. A. Stern and J. A. Johnson III, *Phys. Rev. Lett.* **34**, 1548 (1975).

⁴D. Hill, S. Fornaca, and M. Wickham, *Rev. Sci. Instrum.* **54**, 309 (1983).

⁵R. F. Boivin and E. E. Scime, *Rev. Sci. Instrum.* **74**, 4352 (2003).

⁶I. D. Sudit and F. F. Chen, *Plasma Sources Sci. Technol.* **3**, 162 (1994).

⁷I. H. Hutchison, *Principles of Plasma Diagnostics* (Cambridge University Press, Cambridge, 1987).

⁸E. E. Scime *et al.*, *Phys. Plasmas* **7**, 2157 (2000).

⁹Hamamatsu Co., Technical Datasheets, <http://www.usa.hamamatsu.com>

¹⁰Ophos Instruments Inc., Product Catalog, <http://www.e-opthos.com>

¹¹R. Koslover and R. McWilliams, *Rev. Sci. Instrum.* **57**, 2441 (1986).

¹²M. Zintl and R. McWilliams, *Rev. Sci. Instrum.* **65**, 2574 (1994).

¹³M. Zintl, R. McWilliams, and N. Wolf, *Phys. Plasmas* **2**, 4432 (1995).

¹⁴Lenox Fugle, Inc., Product Catalog, <http://www.brotherselectronics.com>

¹⁵V. A. Godyak, R. B. Piejak, and B. M. Alexandrovich, *Plasma Sources Sci. Technol.* **11**, 525 (2002).

¹⁶M. Lieberman and A. J. Lichtenberg, *Principles of Plasma Discharges and Materials Processing* (Wiley, New York, 1994).

¹⁷M. Light, F. F. Chen, and P. L. Colestock, *Phys. Plasmas* **8**, 4675 (2001).